Available online at www.sciencedirect.com
SCIENCE DIRECT
Journal of Asian Earth Sciences 27 (2006) 230–240
Journal of Asian Earth Sciences
www.elsevier.com/locate/jaes

Mesozoic adakitic rocks from the Xuzhou–Suzhou area, eastern China: Evidence for partial melting of delaminated lower continental crust

Wen-Liang Xu[a,*], Qing-Hai Wang[a], Dong-Yan Wang[a], Jing-Hui Guo[b], Fu-Ping Pei[a]

[a] *College of Earth Sciences, Jilin University, 2199 Jianshe Street, Changchun 130061, People's Republic of China*
[b] *Institute of Geology and Geophysics, Chinese Academy of Sciences, Beijing, 100029, People's Republic of China*

Received 20 July 2004; revised 15 February 2005; accepted 23 March 2005

Abstract

Adakitic rocks in the Xuzhou–Suzhou area, eastern China, consist of dioritic and monzodioritic porphyries and were dated at 131–132 Ma by the SHRIMP U–Pb zircon method. These rocks have high MgO content (1.47–5.73%), high $Mg^{\#}$ values (0.49–0.61), and high La/Yb and Sr/Y ratios. These features are similar to rocks derived from partial melting of a subducted oceanic slab. However, their high initial $^{87}Sr/^{86}Sr$ (0.7053–0.7075) and low $\varepsilon_{Nd}(t)$ values (-4.43 to -13.14) are inconsistent with the origin from slab melting. These rocks often contain garnet residual crystals and eclogite, garnet clinopyroxenite, and garnet amphibolite xenoliths. Petrographical characteristics and estimated P–T conditions of these xenoliths indicate that they were once deeply subducted and subsequently underwent rapid exhumation in the early Mesozoic. Garnet residual crystals from the porphyries show similar chemical compositions to garnets from garnet clinopyroxenite and garnet amphibolite xenoliths. Ages of the inherited zircons of the xenoliths and their host rocks likely indicate that sources for the adakitic magma and protoliths of the eclogite and garnet clinopyroxenite xenoliths in the study area were from Precambrian basement of the North China Craton. The data also suggest that the lower continental crust in the eastern North China Craton was thickened during the early Mesozoic and delaminated in the early Cretaceous. The high-Mg adakitic magma resulted from partial melting of this delaminated lower continental crust and its subsequent interaction with the mantle during upward transport, leaving garnet as the residual phase.

Keywords: Adakite; Xenolith; Delaminated continental crust; Partial melting; Eastern China

1. Introduction

It is known that adakites can be produced by partial melting of the subducted oceanic slab (termed 'slab melting', Defant and Drummond, 1990) in subduction zones. Nevertheless, alternative models for the petrogenesis of adakites have also been proposed, e.g. melting at the base of tectonically thickened crust (Atherton and Petford, 1993; Barnes et al., 1996; Kay and Kay, 2002), assimilation-fractional crystallization (AFC) processes involving a basaltic magma (Castillo et al., 1999), and partial melting of the underplated basaltic lower crust (Rapp et al., 2002) or delaminated lower continental crust (Xu et al., 2002a; Gao et al., 2004). Experimental studies have also suggested that melting of mafic material produces adakitic magmas at about 1.2 GPa pressure, with the residual phase containing garnet but no plagioclase (Rapp and Watson, 1995; Rapp et al., 1999, 2002). Although most well-known adakites are distributed in intraoceanic island arc settings and continental arcs, such as the Andes (Atherton and Petford, 1993; Barnes et al., 1996; Kay and Kay, 2002; Rapp et al., 2002), adakitic rocks within cratons have also been reported, such as those from eastern China (Zhang et al., 2001; Pan et al., 2001; Xu et al., 2001, 2002a; Gao et al., 2004). It is still controversial whether partial melting of the lower continental crust can produce adakitic magma along continental margin or continent–continent collisional tectonic settings.

In this paper, we present petrological, geochemical, and Nd–Sr isotopic data for adakitic rocks and their eclogite xenoliths exposed in the Xuzhou–Suzhou area and further propose a genetic model for these adakitic intrusive rocks.

* Corresponding author. Tel.: +86 431 8502080; fax: +86 431 8502617.
E-mail address: xuwl261@sina.com (W.-L. Xu).

1367-9120/$ - see front matter © 2005 Published by Elsevier Ltd.
doi:10.1016/j.jseaes.2005.03.005

2. Geological setting

The Xuzhou–Suzhou area is located along the southeastern margin of the North China Craton (NCC), about 100 km west of the Tan-Lu fault zone on the southwestern end of the Su–Lu orogen and about 300 km north of the Dabie orogen (Fig. 1). The deformed Neoproterozoic to late Paleozoic strata in the region constitute a Xu(zhou)-Huai(nan) structural nappe (Wang et al., 1998), intruded by several small intrusives named the Liguo, Banjing and Jiagou intrusions from north to south (Fig. 1). They are mainly composed of dioritic porphyry and monzodioritic porphyry. These intrusives were not subjected to structural deformation, but were chiefly controlled by extensional faults (Lin et al., 2000). The uppermost strata intruded by the intrusives in the Xu-Huai nappe are late Permian in age, indicating emplacement after the late Permian. SHRIMP zircon U–Pb ages for the Liguo dioritic porphyry and the Jiagou monzodioritic porphyry are 131.1 ± 3.4 and 132.2 ± 4.1 Ma, respectively (Xu et al., 2004a). Eclogite, garnet-clinopyroxenite and garnet-amphibolite xenoliths, as well as garnet residual crystals, can be found in these Mesozoic intrusives (Xu et al., 2002b).

3. Samples and petrography

Samples used for this study from the Xu-Huai area are hornblende (Hb) dioritic porphyry (the Liguo intrusion), dioritic porphyry (the Banjing intrusion), and monzodioritic porphyry and quartz (Q) monzonitic porphyry (the Jiagou intrusion) (Table 1). These rocks all show porphyritic texture with phenocryst contents of 10–30 vol%. The phenocrysts consist dominantly of zoned hornblende and plagioclase (Fig. 2(a)), implying a magmatic origin. The groundmasses are composed of hornblende, plagioclase and minor orthoclase and quartz.

Abundant xenoliths such as eclogite, garnet clinopyroxenite, garnet amphibolite and garnet residual crystals have been found in these porphyries. The xenoliths occur in the ellipsoidal form, ranging from about 8×10 cm^2 (Fig. 2(b)) to 0.5×1.0 cm^2 in size. A narrow reaction rim of amphibole is frequently observed between the xenolith and the host rock.

Eclogite xenoliths are medium-coarse grained and consists of garnet, omphacite, quartz, and rutile. Primary amphibole occasionally exists in some eclogite xenoliths (Fig. 2(c)). The retrograde amphiboles often occur around clinopyroxene and garnet. Their pleochroism is light yellow-brown and yellow-

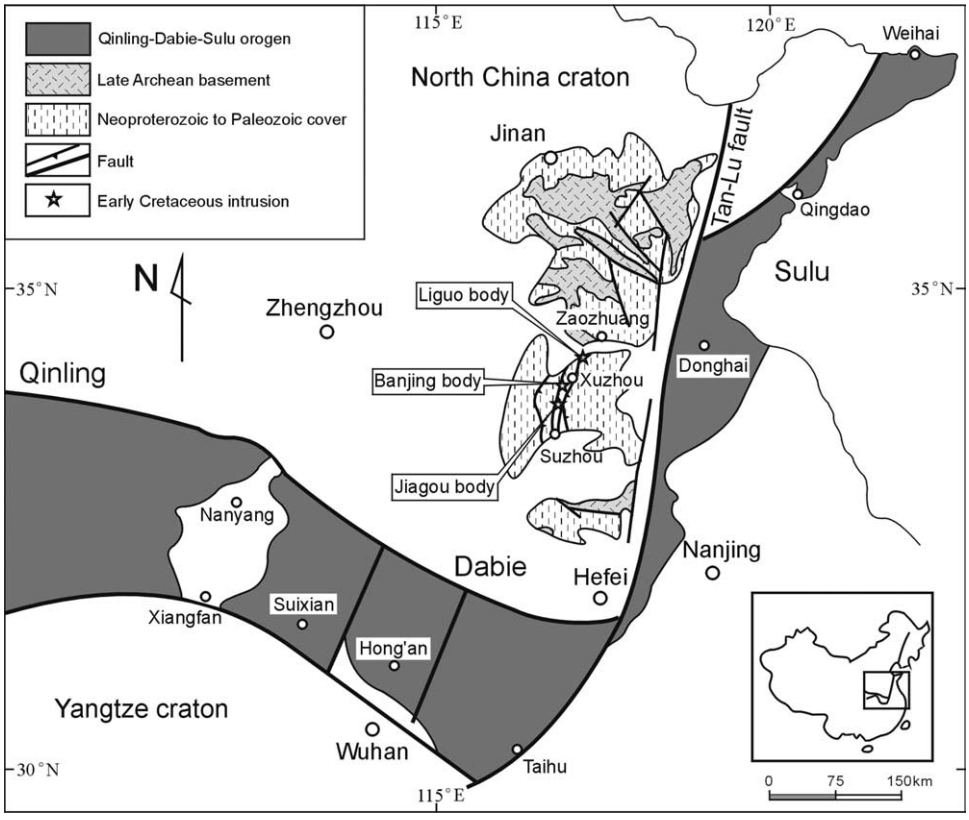

Fig. 1. Tectonic map of the Qinling–Dabie–Sulu collisional belt, showing the distribution of the early Cretaceous intrusives and eclogite xenoliths in the Xuzhou–Suzhou area, eastern China.

Table 1
Major (wt%), trace element (ppm) and Sr–Nd isotopic data of the Mesozoic intrusive rocks in the Xuzhou–Suzhou area

Locality	Liguo			Banjing						Jiagou
Sample no.	L-7	LG1-1	LG3-8	064-1	8102-389	8201-69-10	8201-69-2	8202-392	074	J-25
Latitude	34°33′03″	34°34′26″	34°33′07″	34°08′58″	34°09′48″	34°09′50″	34°09′45″	34°09′40″	34°08′55″	33°52′42″
Longitude	117°19′03″	117°18′55″	117°18′00″	117°05′40″	117°04′25″	117°04′22″	117°04′30″	117°04′42″	117°05′38″	117°00′54″
Rock type	D–P		Q-M-P	M–D–P	Q–M–P	Hb–D–P	M–D–P	D–P		M–D–P
SiO_2	60.88	60.74	67.18	59.08	66.57	55.33	61.73	60.7	60.58	61.41
TiO_2	0.61	0.62	0.30	0.62	0.34	0.83	0.47	0.61	0.60	0.58
Al_2O_3	14.34	13.69	14.63	17.57	15.23	16.8	17.14	14.85	14.84	15.06
Fe_2O_3	3.14	2.83	1.11	3.25	1.55	3.88	1.93	2.87	2.52	2.29
FeO	3.34	3.92	1.75	2.37	2.15	4.33	1.93	3.80	3.53	4.03
MnO	0.11	0.12	0.07	0.08	0.09	0.14	0.06	0.14	0.09	0.11
MgO	4.68	5.73	1.47	2.88	2.34	4.71	3.05	4.59	4.59	3.44
CaO	5.58	5.43	3.10	4.88	3.25	7.33	4.69	5.68	4.43	5.54
Na_2O	5.12	3.71	4.69	5.1	5.16	3.95	5.43	4.05	4.42	4.28
K_2O	0.89	2.12	2.62	2.37	2.57	1.14	2.21	1.73	2.17	2.28
P_2O_5	0.16	0.18	0.09	0.24	0.12	0.25	0.15	0.17	0.16	0.17
LOI	0.93	0.68	2.75	2.06	0.35	1.25	1.03	0.55	2.38	0.49
Total	99.78	99.77	99.76	100.5	99.72	99.94	99.82	99.74	100.3	99.68
$Mg^{\#a}$	58	61	49	49	54	52	60	56	59	50
La	14.25	18.25	11.45	26.25	16.59	16.90	21.58	18.39	14.68	25.85
Ce	32.32	38.33	25.33	56.77	32.81	41.31	42.67	37.77	32.37	58.98
Pr	4.21	5.00	3.46	6.78	4.21	5.39	4.78	4.87	3.94	5.41
Nd	17.41	19.31	13.92	26.03	16.30	22.26	17.26	18.36	16.19	20.33
Sm	3.66	3.70	2.88	4.57	3.19	4.35	2.95	3.40	3.18	4.11
Eu	1.11	0.94	0.73	1.27	0.82	1.17	0.94	0.94	0.90	1.25
Gd	3.46	2.92	2.01	3.28	2.14	3.65	2.26	2.86	2.69	3.51
Tb	0.50	0.43	0.24	0.46	0.28	0.52	0.31	0.44	0.37	0.49
Dy	2.84	2.30	1.05	2.54	1.33	3.11	1.72	2.39	2.21	2.73
Ho	0.54	0.44	0.17	0.48	0.24	0.60	0.33	0.47	0.43	0.53
Er	1.58	1.16	0.48	1.39	0.67	1.78	0.90	1.30	1.15	1.58
Tm	0.22	0.17	0.08	0.22	0.10	0.27	0.14	0.20	0.18	0.22
Yb	1.45	1.11	0.48	1.29	0.70	1.65	0.89	1.30	1.13	1.52
Lu	0.19	0.17	0.08	0.21	0.14	0.27	0.15	0.21	0.18	0.21
Y	14.41	11.83	4.84	13.83	7.01	17.6	9.23	13.16	12.67	14.64
Rb	13.17	65.43	64.63	51.8	52.5	28	39.9	49.4	49.2	62.21
Sr	617.8	510	452	841	861	629	1052	616	535	1180
Ba	408.9	592	827	704	886	575	1264	664	567	1578
Nb	3.00	4.48	2.36	7.3	3.23	6.7	5.2	4.27	5.9	6.12
Ta	–	0.33	0.14	–	0.22	–	–	0.28	–	0.11
Zr	69.88	53.61	99.81	142	113	106	117	127.8	106	192.9
Hf	2.19	1.49	3.18	–	3.08	–	–	3.14	–	5.55
Th	2.78	4.86	3.44	2.0	3.88	10.2	2.0	3.51	–	8.07
U	1.14	1.27	1.31	–	1.42	–	–	0.93	7.9	3.61
Sc	18.32	15.75	4.71	–	6.06	–	–	14.9	–	17.0
V	208.9	116.6	55.15	–	69.4	–	–	132.2	–	133.2
Cr	214.30	228.3	66.65	–	116.5	59	96	187	157	106.3
Co	25.86	25.32	7.93	35	11.28	–	–	23.84	–	19.01
Ni	103.73	133.5	25.18	16.3	44.82	22.9	42.2	80.72	82.9	35.37
$(La/Sm)_N$	2.52	3.19	2.57	3.72	3.36	2.52	4.74	3.50	2.99	4.07
$(La/Yb)_N$	6.84	11.42	16.60	14.13	16.55	7.11	16.84	9.85	9.02	11.78
Sr/Y	42.9	43.1	93.6	60.8	122.9	35.7	114	46.8	42.2	80.6
$^{87}Rb/^{86}Sr$	0.199	0.39	0.407		0.184		0.097	0.215		0.141
$^{87}Sr/^{86}Sr$	0.707519	0.706250	0.706950		0.705685		0.706000	0.706416		0.707738
$2\sigma(\times10^{-6})$	22	20	14		15		19	18		14
$^{147}Sm/^{144}Nd$	0.1248	0.1207	0.1339		0.1252		0.1093	0.1195		0.1168
$^{143}Nd/^{144}Nd$	0.512117	0.512248	0.512346		0.512349		0.511889	0.512047		0.512030
$2\sigma(\times10^{-6})$	8	11	10		8		10	9		8
I_{Sr} (132 Ma)	0.7071	0.7055	0.7062		0.7053		0.7058	0.7060		0.7075
ε_{Nd}(132 Ma)[b]	−8.95	−6.33	−4.64		−4.43		−13.14	−10.23		−10.52
T_{DM} (Ma)[b]	1766	1476	1533		1378		1836	1780		1757
$f_{Sm/Nd}$	−0.37	−0.39	−0.32		−0.36		−0.44	−0.39		−0.41

– Not determined and/or below detecting limit; D-P, dioritic porphyry; Hb-D-P, hornblende-dioritic porphyry; M-D-P, Monzodioritic porphyry; Q-M-P, Quartz monzonitic porphyry.

[a] Mg= molar 100 $(Mg/Mg+Fe^{2+})$, where $FeO=FeO+0.9\ Fe_2O_3$.

[b] The present-day $^{143}Nd/^{144}Nd$ and $^{147}Sm/^{144}Nd$ values used are 0.512638 and 0.1967 for chondrite and 0.51315 and 0.222 for depleted mantle.

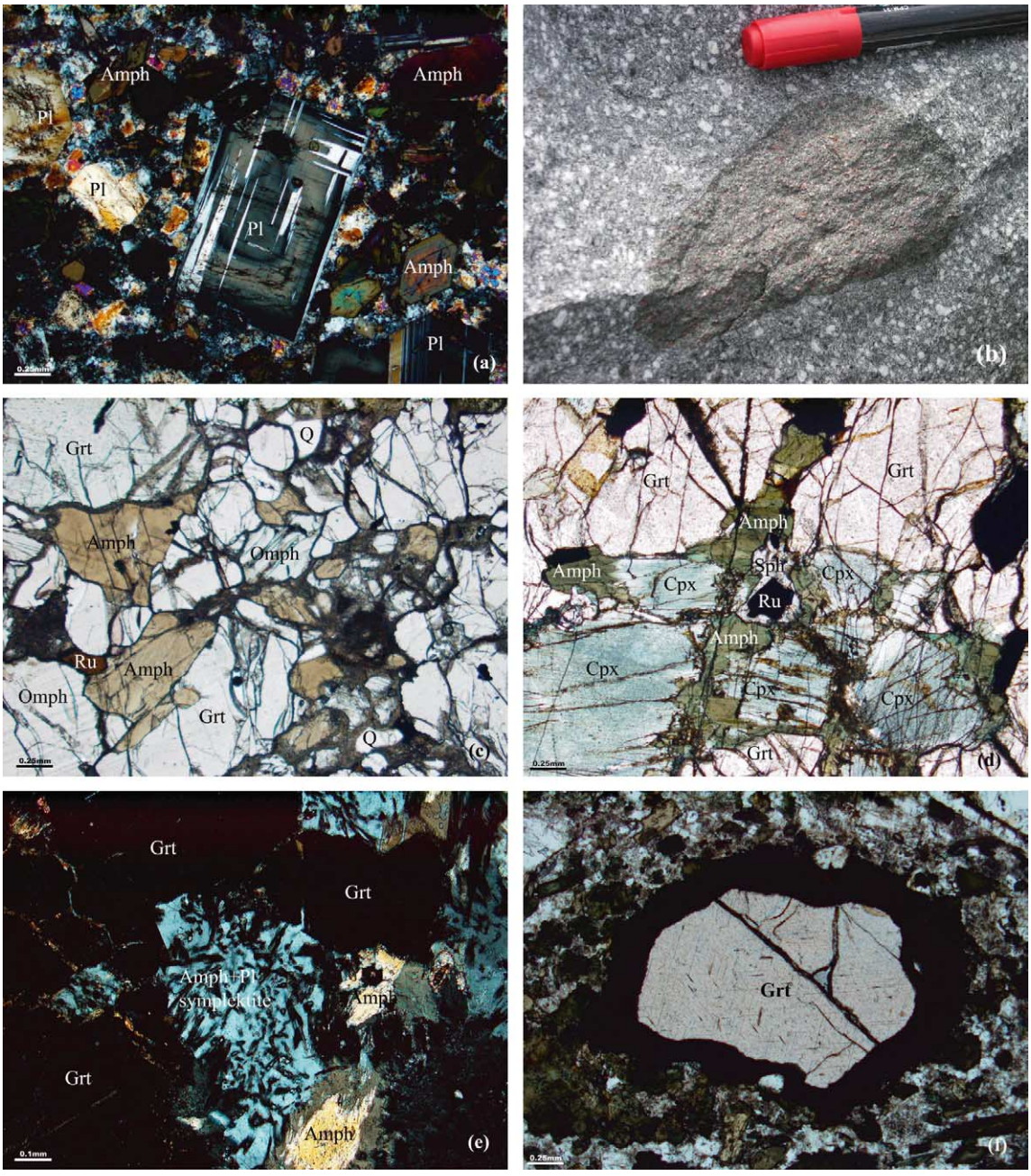

Fig. 2. Photographs showing field occurrences and textures of the host rocks and xenoliths. (a) Zoned plagioclase phenocryst in monzodioritic porphyry (crossed polarizing); (b) Field occurrence of the eclogite xenolith; (c) Primary amphibole in eclogite xenolith (plane polarizing); (d) Capped sphene around rutile in the garnet clinopyroxenite xenolith (plane polarizing). (e) Amphibole + plagioclase symplectite in the garnet clinopyroxenite (crossed polarizing). (f) Garnet residual crystal in the monzodioritic porphyry (plane polarizing).

green, respectively, under a plane polarizing microscope. Capped sphene occurs around rutile (Fig. 2(d)).

Garnet clinopyroxenite xenoliths are medium- to coarse-grained and have a garnet + clinopyroxene + rutile assemblage. The amphibole + plagioclase symplectite and retrograde amphiboles around clinopyroxenes and garnets commonly occur in garnet clinopyroxenite (Fig. 2(e)), showing amphibolite-facies retrograde metamorphism.

Garnet residual crystals and sometimes rutile are present in the host rocks. A 0.1–0.3 mm wide resorption rim of cryptocrystalline material formed around the garnet residual crystal (Fig. 2(f)).

4. Analytical methods

Whole-rock major element analysis of fresh porphyry samples was determined by XRF at the Hubei Geological Analytical Center in Wuhan. The analytical uncertainties range from 1 to 3%. FeO was determined using

the traditional wet chemical method. Trace element compositions of six samples (L-7, LG1-1, LG3-8, 8102-389, 8201-392, J-25) were analyzed by ICP-MS at Guangzhou Institute of Geochemistry, Chinese Academy of Sciences, while those of the other four samples (064-1, 8201-69-10, 8201-69-2, 074) were analyzed by ICP-AES at the Hubei Geological Analytical Center in Wuhan. The ICP-MS analytical procedure has been outlined by Liu et al. (1996). Whole-rock Sr and Nd isotopic compositions were analyzed on a VG354 thermal ionization mass spectrometer (TIMS) at the Institute of Geology and Geophysics, Chinese Academy of Sciences. Details for chemical separation and isotopic measurement can be found in Qiao et al. (1987, 1990).

Mineral compositions of the xenoliths were analyzed by a Cameca-Camebax SX15 wavelength-dispersive electron microprobe at the Institute of Geology and Geophysics, Chinese Academy of Sciences. The operating conditions were 15 kV accelerating voltage, 12 nA beam current and 1 μm beam size. The counting time at each peak was 20 s. Natural silicates and oxides were used as standards.

5. Analytical results

5.1. Major and trace element data

Major and trace element concentrations for the intrusive rocks are given in Table 1 and are plotted in Figs. 3–8. Major element compositions show that the intrusives exposed in the Xuzhou–Suzhou region are mainly diorite and granodiorite and their SiO_2 contents range from 55.3 to 67.2 wt%. The An–Ab–Or classification plot based on the CIPW norm of granitoid indicates that most of them are tonalite (Fig. 3). They are subalkaline based on the alkali versus silica plot (Fig. 4) and show a calc-alkaline evolutionary trend in the AFM diagram (not shown in the text). Their K_2O/Na_2O ratios range from 0.17 to 0.57, indicating Na_2O enrichment. Their K_2O contents (0.89–2.62 wt%) normally are higher than typical adakites derived from slab melting (Defant and Drummond, 1990), and belong to the medium-potassic calc-alkaline series (Gill, 1981). These rocks have relatively high MgO contents (1.47–5.73 wt%). Their $Mg^{\#}$ values ($Mg^{\#}$ = molar [Mg/(Mg + Fe^{2+})]; 0.49–0.61) are similar to those of adakites derived from slab melting but considerably higher than experimental melts from hydrous basalt in the garnet stability field and Archean tonalite–trondhjemite–diorite (TTD) (Fig. 5).

Chondrite-normalized rare earth element (REE) patterns of the intrusive rocks are characterized by (1) enrichment in light rare earth element (LREE), (2) depletion in heavy REE (HREE), and (3) slightly negative or no Eu-anomaly (Fig. 6). Their REE total amounts vary between 62.4 and 131.5 ppm. In the primitive mantle (PM) normalized trace

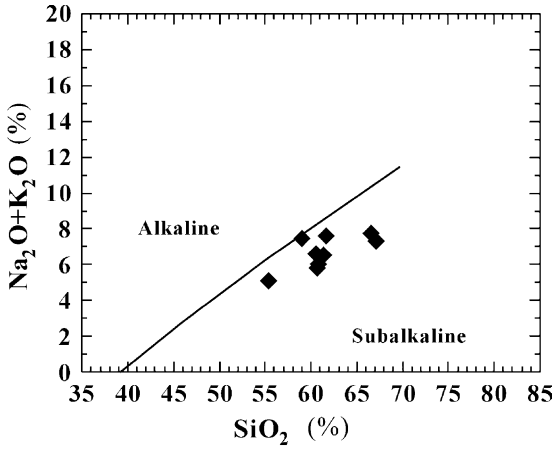

Fig. 4. SiO_2 vs. (Na_2O+K_2O) diagram for the Xuzhou–Suzhou adakitic intrusive rocks. The boundary between the alkaline and subalkaline field is after Irvine and Baragar (1971).

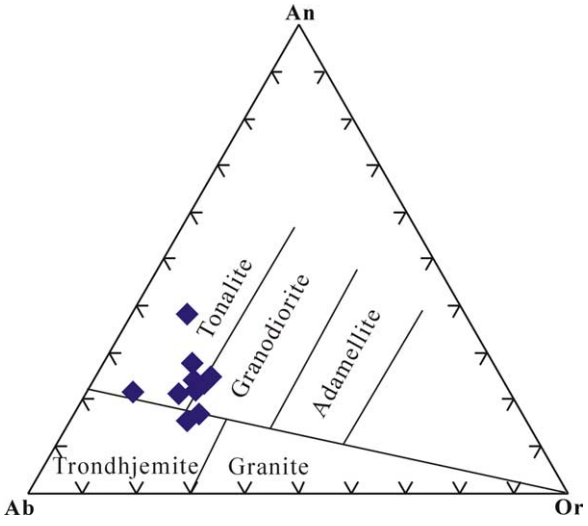

Fig. 3. An–Ab–Or classification diagram based on the CIPW norm for the Xuzhou–Suzhou adakitic intrusive rocks.

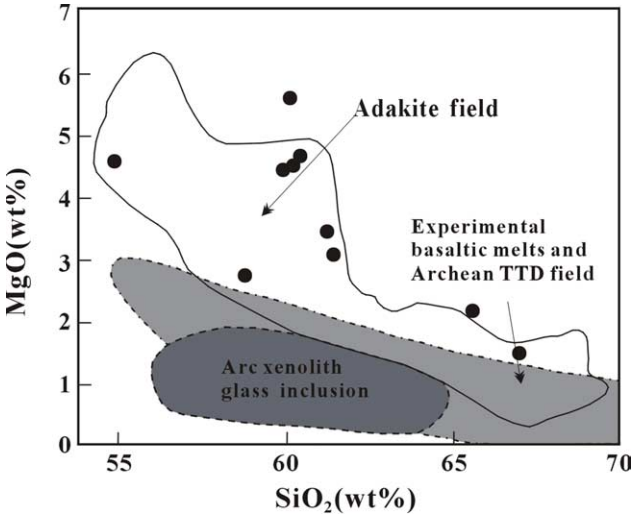

Fig. 5. MgO vs. SiO_2 diagram for the Xuzhou–Suzhou adakitic intrusive rocks (after Defant and Kepezhinskas, 2001).

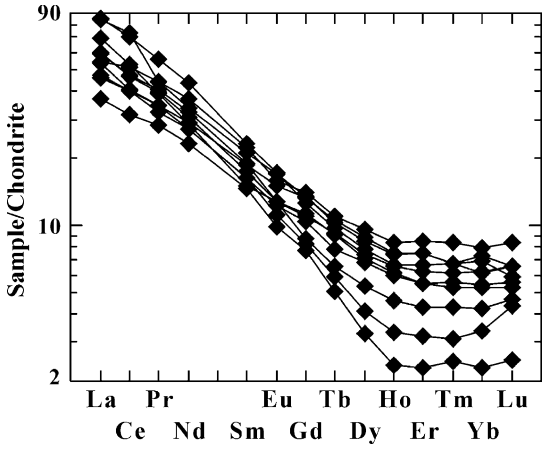

Fig. 6. Chondrite-normalized REE patterns of the early Cretaceous intrusives in the Xuzhou–Suzhou area.

element spider diagram (Fig. 7), these intrusive rocks show a remarkable depletion in high field strength element (HFSE; Nb, Ta, Y and Yb), and enrichment in large ion lithophile elements (LILE) relative to LREE and HFSE. They show high La_N/Yb_N (6.8–16.8) and Sr/Y (35.7–122.9) ratios as well as low Y (4.84–17.6 ppm) and Yb (0.48–1.65 ppm) contents. These samples, therefore, fall in the adakite and high-Al TTD field when plotted in a Sr/Y versus Y diagram (Fig. 8). These characteristics are similar to slab melts (Defant and Drummond, 1990).

5.2. Sr–Nd isotopes

Initial $^{87}Sr/^{86}Sr$ ratios at 132 Ma for the intrusive rocks are relatively uniform (0.7053–0.7075; Table 1), whereas their Nd isotopic compositions are heterogeneous. The $\varepsilon_{Nd}(t)$ values at 130 Ma range from −4.43 to −13.14 (Fig. 9), which are distinctly different from slab melts (Defant and Drummond, 1990), but similar to those of adakite rocks derived from partial melting of the lower continental crust (Petford and Atherton, 1996)

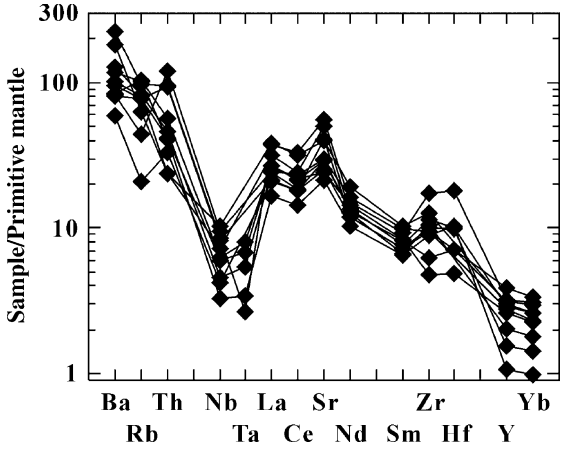

Fig. 7. Primitive mantle (PM)—normalized trace element spider diagrams of the early Cretaceous intrusives from the Xuzhou–Suzhou area.

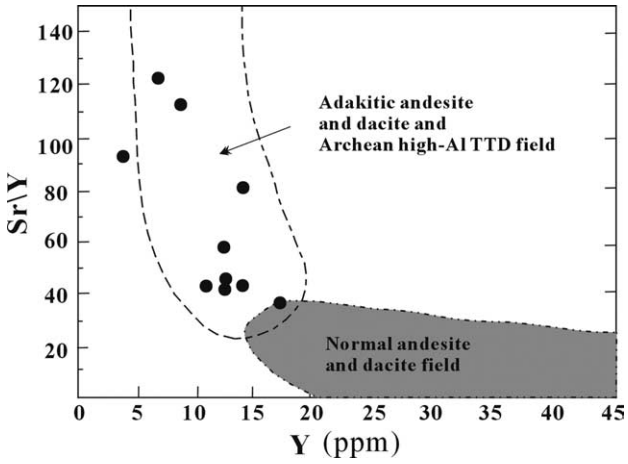

Fig. 8. Y vs. Sr/Y diagram for the Xuzhou–Suzhou adakitic intrusive rocks (after Defant and Kepezhinskas, 2001).

and delaminated lower continental crust (Xu et al., 2002a). In terms of the Sr–Nd isotopic compositions, most samples fall in the mantle array and are similar to those of Mesozoic mafic intrusive rocks from the Dabie orogen (Jahn et al., 1999; Li et al., 1998). The relatively high initial $^{87}Sr/^{86}Sr$ ratios and low $\varepsilon_{Nd}(t)$ values of the intrusions imply that crustal contamination could have played a role during their emplacement and crystallization. This is supported by their high K_2O contents, depletions in HFSE and enrichments in LILE. All samples have Mesoproterozoic and Paleoproterozoic T_{DM}, ranging from 1378 to 1836 Ma (Table 1), which also suggests an old source for the adakitic magma.

5.3. Mineral chemistry of the xenoliths

Electron microprobe analyses of garnet, clinopyroxene and amphibole in the xenoliths are shown in Table 2. The garnet has 27–45 mol% pyrope, 35–54 mol%

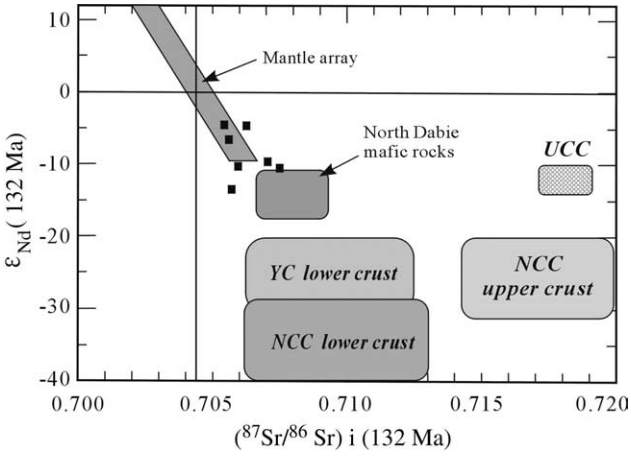

Fig. 9. Initial $(^{87}Sr/^{86}Sr)_i$ vs. ε_{Nd} (132 Ma) diagram for the intrusive rocks from the Xuzhou–Suzhou area. Sr–Nd isotopic data sources: the NCC lower crust and upper crust (Jahn et al., 1999); the YC lower crust (Chen and Jahn, 1998); the north Dabie mafic rocks (Jahn et al., 1999; Li et al., 1998); the UCC (Jahn et al., 1988).

Table 2
Electron microprobe analyses of garnet, clinopyroxene and amphibole in the xenoliths (%)

Type	Eclogite (B1-10)			Eclogite (603-2-2)			Grt-clinopyroxenite (JG1-8)			Reaction rim(JG1-8)	Residual crystal	Grt-amphibolite (J-21)	
Latitude	34°08′58″			34°08′55″			33°52′42″				33°52′44″	33°52′45″	
Longitude	117°05′40″			117°05′42″			117°00′54″				117°00′51″	117°00′53″	
Mineral	Grt	Omph	Am[b]	Grt	Omph	Am[a]	Grt	Cpx	Am[a]	Am	Grt(J-11)	Grt	Am
SiO_2	40.96	54.70	43.75	39.56	52.94	40.56	38.53	53.57	44.67	44.75	39.03	39.61	44.31
TiO_2	0.00	0.45	0.75	0.00	0.31	2.36	0.15	0.18	1.48	0.53	0.09	0.05	1.19
Al_2O_3	22.97	9.83	16.63	22.50	8.84	16.37	23.70	3.13	11.96	14.86	21.70	23.10	14.63
Cr_2O_3	0.08	0.00	0.14	0.00	0.06	0.04	0.03	0.20	0.33	0.07	0.07	0.00	0.04
FeO	15.71	4.20	5.77	19.90	5.37	13.77	24.27	6.63	12.98	14.44	25.47	21.88	11.47
MnO	0.18	0.02	0.07	0.47	0.00	0.07	0.59	0.07	0.00	0.19	0.45	0.47	0.00
MgO	12.44	11.56	16.45	9.09	11.38	11.71	6.75	14.45	12.90	10.70	7.68	9.57	14.21
CaO	7.57	15.40	10.38	9.13	17.20	10.18	6.08	20.86	10.33	10.21	6.36	5.24	9.63
Na_2O	0.09	3.85	3.28	0.00	3.90	2.72	0.00	0.92	2.54	0.99	0.00	0.08	2.57
K_2O	0.00	0.00	0.81	–	0.00	0.23	–	0.00	1.02	1.19	–	–	0.64
Total	100.01	100.01	98.03	100.65	100.0	98.01	100.07	100.01	98.21	97.93	100.80	100.03	98.69
Si	3.029	1.965	6.195	2.994	1.906	5.815	2.944	1.969	6.437	6.400	3.006	2.979	6.178
Ti	0.000	0.012	0.080	0.000	0.008	0.255	0.009	0.005	0.160	0.057	0.005	0.003	0.125
Al	2.000	0.416	2.773	2.006	0.375	2.759	2.133	0.135	2.030	2.503	1.968	2.047	2.402
Cr	0.005	0.000	0.016	0.000	0.002	0.005	0.002	0.006	0.038	0.008	0.004	0.000	0.004
Fe^{3+}	0.000	0.000	0.000	0.055	0.065	1.167	0.000	0.000	0.651	0.953	0.059	0.000	1.303
Fe^{2+}	0.971	0.126	0.684	1.204	0.097	0.484	1.607	0.204	0.913	0.774	1.581	1.434	0.035
Mn	0.011	0.001	0.008	0.030	0.000	0.009	0.038	0.002	0.000	0.023	0.029	0.030	0.000
Mg	1.371	0.619	3.473	1.026	0.611	2.503	0.769	0.792	2.771	2.281	0.882	1.073	2.953
Ca	0.600	0.593	1.575	0.740	0.664	1.564	0.498	0.821	1.595	1.565	0.525	0.422	1.439
Na	0.013	0.268	0.901	0.000	0.272	0.756	0.000	0.066	0.710	0.275	0.000	0.012	0.694
K	0.000	0.000	0.146	–	0.000	0.042	–	0.000	0.188	0.217	–	–	0.114
Alm	35			40			54				52	49	
And	4			3			0				3	0	
Gro	16			22			18				15	14	
Pyr	45			34			27				29	36	
Spe	0			1			1				1	1	
WEF		71			72			93					
Jd		29			23			7					
Ae		0			5			0					

Formulae are based on 12O, 6O and 23O, respectively. – Below detection limit.

[a] Retrograded amphibole in the xenoliths.

[b] Primary amphibole in eclogite xenolith.

almandine, and 14–22 mol% grossular. Andradite and spessartine components are generally less than 4 and 1%, respectively. Garnets in the eclogite are similar to those in the B-type eclogite (Coleman et al., 1965), while garnets in garnet clinopyroxenites are transitional between B- and C-type eclogites (Xu et al., 2002b).

Clinopyroxenes in eclogite xenoliths are omphacite with 23–29 mol% jadeite, while those in garnet clinopyroxenite are augites with 7 mol% jadeite (Table 2).

Following the Leake's amphibole classification (Leake et al., 1997), amphiboles in eclogite, garnet clinopyroxenite, and garnet amphibolite xenoliths are calcium amphiboles. Primary amphibole in eclogite (sample B1-10) is pargasite, which is rich in Al, Na, and Mg (Table 2). However, retrograded amphiboles in eclogite (sample 603-2-2) and garnet clinopyroxenite (sample JG1-8) are ferroan pargasite and edenitic hornblende, which are rich in Fe and Si, respectively (Table 2). Amphibole in garnet amphibolite (sample J-21) is pargasitic hornblende. Compared to the primary and retrograde amphiboles in eclogite and garnet clinopyroxenite, amphiboles occurring in the reaction rim are rich in FeO and K_2O, and poor in Na_2O, MgO, and TiO_2, and are tschermakitic hornblendes.

6. Discussion

6.1. Genesis of the adakitic rocks

As discussed above, adakites may form in different ways such as slab melting (Defant and Drummond, 1990), melting at the base of tectonically thickened crust, melting within a subduction-erosion regime (Kay and Kay, 2002), melting of delaminated lower continental crust (Xu et al., 2002a; Kay and Kay, 2002; Gao et al., 2004), and assimilation-fractional crystallization (AFC) processes involving basaltic magma (Castillo et al., 1999). The relatively high K_2O content, enrichments in LILE and LREE, depletions in HFSE (Fig. 7), and high initial $^{87}Sr/^{86}Sr$ ratios and low $\varepsilon_{Nd}(t)$ values of the Xuzhou–Suzhou porphyries do not favor a slab-melting model. This conclusion is supported by the presence of inherited zircon ages of 1700–1800 and 2400–2550 Ma in these porphyries, as dated by the SHRIMP U–Pb method (Xu et al., 2004a). In addition, there are no co-existing mafic rocks associated with these adakitic rocks in the Xuzhou–Suzhou area. This implies that the adakitic rocks could not have been produced by an AFC process involving basaltic magma (Castillo et al., 1999).

We suggest that the Xuzhou–Suzhou adakitic rocks resulted from partial melting of the delaminated lower continental crust. Experimental results on melting of mafic rocks indicate that adakitic magma derived directly from partial melting of basaltic lower crust should have a relatively low MgO content (Rapp and Watson, 1995). In contrast, the Xuzhou–Suzhou adakitic rocks have higher MgO content and higher $Mg^{\#}$ values, high initial $^{87}Sr/^{86}Sr$ ratios and low $\varepsilon_{Nd}(t)$ values that are inconsistent with simple melting of mafic rocks in the lower crust (Defant and Kepezhinskas, 2001). The Xuzhou–Suzhou adakitic rocks are quite similar to the Late Jurassic Xinglonggou high-Mg adakites and andesites in terms of geochemical and isotopic compositions. The latter two possibly originated as melt derived from melting of delaminated lower crust, followed by subsequent interactions with peridotite during upward transport (Gao et al., 2004). We favor a similar origin for the Xuzhou–Suzhou rocks and suggest that the origin of adakitic magma involved both the lower continental crust and the mantle. The former can be proved by the trace element and Sr–Nd isotopic compositions, while the latter is supported by the high MgO contents of the intrusive rocks. As discussed below, the xenoliths found in these adakitic rocks are the best candidates for delaminated lower crust.

6.2. Xenoliths as the source of the adakitic rocks

As described above, numerous eclogite, garnet clinopyroxenite and garnet amphibolite xenoliths, as well as garnet residual crystals, can be found in Mesozoic intrusive rocks from the Xuzhou–Suzhou area. This implies a possible genetic link between the host rocks and xenoliths and residual crystals. HREE and HFSE depletions in the host rocks are consistent with the presence of garnet residual crystals, suggesting that garnet was the residual phase during partial melting of the source rocks. The chemical composition of the garnet residual crystal in the host rocks is similar to that of the garnet in amphibole-bearing garnet clinopyroxenite and garnet amphibolite xenoliths (Table 2). This suggests that the source of the adakitic rocks might have been retrograde eclogite and garnet clinopyroxenite. The eclogites consist of garnet (34–45 mol% pyrope, 35–40 mol% almandine, and 16–22 mol% grossular), omphacite (23–29 mol% jadeite), quartz, and rutile. This mineralogical characteristics indicate that the xenoliths have undergone eclogite-facies metamorphism at pressures >1.5 GPa and temperature of 709–861 °C (Xu et al., 2002b). It can be seen from Table 2 that there are significant differences in chemical composition between the retrograde amphibole and amphibole in the reaction rim. Such differences demonstrate that amphibole around clinopyroxene (Cpx) in the xenoliths did not result from the reaction between the xenolith and the host magma. The common occurrences of plagioclase + amphibole symplectite in eclogite and garnet clinopyroxenite xenoliths indicate that the amphibole is more likely to be product of amphibolite-facies retrograde metamorphism (Fig. 2(e)), and suggest amphibolite-facies retrograde metamorphism below 0.70–1.03 GPa and 666–738 °C following formation of eclogite (Xu et al., 2002b). The amphibolite-facies retrograde metamorphism may have resulted from cooling and decompression of the host adakitic magma in the middle-lower crust.

6.3. Melting of the delaminated lower continental crust

Inherited zircons from the host rocks show two age peaks of 2400–2550 and 1700–1800 Ma (Xu et al., 2004a), which are similar to those of inherited zircons from the eclogite, garnet clinopyroxenite and gneiss xenoliths (Xu et al., 2004a,b) as well as from granulite xenoliths from the Cenozoic Nushan basalts (Huang et al., 2003). These two age peaks correspond well to the two most significant tectonothermal events of latest Archean and latest Paleoproterozoic time in the NCC (Ma and Bai, 1998; Zhao et al., 2001). The North China Craton and the Yangtze Craton (YC) have distinct Precambrian crustal growth histories. Crustal growth in the YC mainly occurred around 700–800 Ma with only minor Archean and Paleoproterozoic crustal rocks being exposed (Ma and Bai, 1998; Li et al., 1999; Gao et al., 2001; Zheng et al., 2003). We thus propose that the source for the adakitic rocks and the protoliths of the eclogite, Grt-clinopyroxenite, and gneiss xenoliths should belong to the Precambrian NCC basement.

The SHRIMP zircon U–Pb age (206 ± 15 Ma) and whole-rock and garnet Sm–Nd isochron age (219.4 Ma) of an eclogite xenolith indicate that the eclogite-facies metamorphism in the Xuzhou–Suzhou area took place during the Triassic (Xu et al., 2002b, 2004b), and coincide with the peak ultrahigh-pressure metamorphism (UHPM) of the Dabie-Sulu belt (Li et al., 1989; Ames et al., 1993; Yang et al., 2002). We suggest that the eclogite-facies metamorphism recorded in the eclogite xenoliths was related to the UHPM in the Dabie-Sulu belt. Accordingly, it is reasonable to infer that parts of the deep crustal sections along the southeastern margin of the NCC were involved in the Triassic high pressure (HP)/UHP metamorphic event. We propose that the xenoliths in the early Cretaceous adakitic rocks should represent part of the delaminated NCC basement. The Triassic eclogite-facies metamorphism indicates that the lower continental crust of the southeastern margin of the NCC was thickened in the early Mesozoic and that the thickening resulted from deep subduction of the YC towards the NCC in a NWW or NW direction (Xu et al., 2002b). It has been shown by Mesozoic granites that the YC basement can be traced under the southeastern margin of the NCC (Luo and Miao, 2002; Xu et al., 2005). The amphibolite-facies retrograde metamorphism observed in the xenoliths might correspond to quick exhumation of the Dabie-Sulu UHPM rocks (180–200 Ma, Jiang et al., 1999; 175–195 Ma, Wang and Lin, 2002).

The Early Mesozoic break-off of the subducted YC slab and delamination of the thickened NCC lower crust led to upwelling of the asthenosphere and thinning of the lithospheric mantle (e.g. Gao et al., 1998; Wu and Sun, 1999; Xu et al., 2000; Gao et al., 2004). This deep process was manifested by 155–160 Ma magmatism that occurred in a post-orogenic extensional environment in the southeastern NCC (Luo and Miao, 2002; Gao et al., 2004; Xu et al., 2005) and bimodal magmatism around 132–112 Ma in the eastern NCC. Heat flux from the underlying asthenosphere triggered melting of the delaminated eclogite and garnet clinopyroxenite and subsequent generation of the Late Jurassic-Early Cretaceous adakitic magma, which is also prominent in western Liaoning in the northern part of the NCC (Gao et al., 2004).

7. Conclusions

The 132–131 Ma dioritic- and monzodioritic-porphyries from the Xuzhou–Suzhou area show geochemical characteristics of adakites with high MgO content and high La/Yb and Sr/Y ratios. Their Sr–Nd isotopic compositions, together with occurrences of residual garnet crystals and eclogite and garnet clinopyroxenite xenoliths, indicate that the adakitic magma could have been derived from partial melting of delaminated eclogitic lower crust in the NCC. However, the high-Mg character of the intrusive rocks is attributed to interaction of the melt with the mantle. The Early Mesozoic eclogite-facies metamorphism of the NCC lower crust recorded by the eclogite xenolith is related to the UHPM in the Dabie-Sulu belt caused by deep subduction of the Yangtze Craton beneath the North China Craton. Break-off of the subducted Yangtze slab and delamination of the thickened North China lithosphere resulted in upwelling of the asthenosphere. Partial melting of the delaminated eclogite, garnet clinopyroxenite, and garnet amphibolite of the North China lower continental crust generated the adakitic magma, leaving garnet as a residual phase.

Acknowledgements

We sincerely appreciate assistance of the staff members of the following laboratories: the ICP-MS laboratory of Guangzhou Institute of Geochemistry Chinese Academy of Sciences in Guangzhou, the Hubei Geological Analytical Center in Wuhan, and the Laboratory of Radiogenic Isotope Geochemistry and the electron microprobe laboratory of Institute of Geology and Geophysics, Chinese Academy of Sciences in Beijing. We thank Fukun Chen and Shan Gao for helpful suggestions that have significantly improved an earlier version of the manuscript. We also thank Prof Kevin Burke for help to improve the revised manuscript. This study was financially supported by research grants from the Ministry of Science and Technology of China (No. TG1999075502) and from the National Nature Science Foundation of China (No. 40172030 and No. 40133020).

References

Ames, L., Tilton, G.R., Zhou, G.Z., 1993. Timing of collision of the Sino-Korean and Yangtze cratons: U–Pb zircon dating of coesite-bearing eclogites. Geology 21, 339–342.

Atherton, M.P., Petford, N., 1993. Generation of sodium-rich magmas from newly underplated basaltic crust. Nature 362, 144–146.

Barnes, C.G., Petersen, S.W., Kistler, R.W., Murray, R., Kay, M.A., 1996. Source and tectonic implications of tonalite-trondhjemite magmatism in the Klamath Mountains. Contributions to Mineralogy and Petrology 123, 40–60.

Castillo, P.R., Janney, P.E., Solidum, R.U., 1999. Petrology and geochemistry of Camiguin Island, southern Philippines: insights to the source of adakites and other lavas in a complex arc setting. Contributions to Mineralogy and Petrology 134, 33–51.

Chen, J.F., Jahn, B.M., 1998. Crustal evolution of southeastern China: Nd and Sr isotopic evidence. Tectonophisics 284, 101–133.

Coleman, R.G., Lee, L.D., Beaty, L.B., Brannock, W.W., 1965. Eclogites and eclogites: Their differences and similarities. Geology Society American Bulletin 76, 483–508.

Defant, M.J., Drummond, M.S., 1990. Derivation of some modern arc magmas by melting of young subducted lithosphere. Nature 347, 662–665.

Defant, M.J., Kepezhinskas, P., 2001. Evidence suggests slab melting in arc magmas. EOS (Transactions, American Geophysical Union) 82, 65–69.

Gao, S., Zhang, B.-R., Jin, Z.-M., Kern, H., Luo, T.-C., Zhao, Z.-D., 1998. How mafic is the lower continental crust? Earth and Planetary Science Letters 161, 101–117.

Gao, S., Qiu, Y., Ling, W., McNaughton, N.J., Groves, D.I., 2001. SHRIMP single zircon U–Pb dating of the Kongling high-grade metamorphic terrain: evidence for 3.2 Ga old continental crust in the Yangtze craton. Science in China (Series D) 44, 326–335.

Gao, S., Rudnick, R.L., Yuan, H.L., Liu, X.M., Liu, Y.S., Xu, W.L., Ling, W.L., Ayers, J., Wang, X.C., Wang, Q.H., 2004. Recycling lower continental crust in the North China craton. Nature 432, 892–897.

Gill, J.B., 1981. Orogenic andesite and plate tectonics. Springer, Berlin p. 358.

Huang, X.L., Xu, Y.G., Liu, D.Y., Jian, P., 2003. Paleoproterozoic lower crust beneath Nushan in Anhui Province: evidence from zircon SHRIMP U–Pb dating on granulite xenoliths in Cenozoic alkali basalt. Chinese Science Bulletin 48, 1381–1385.

Irvine, T.N., Baragar, W.R.A., 1971. A guide to the chemical classification of the common volcanic rocks. Canadian Journal of Earth Science 8, 523–548.

Jahn, B.M., Auvray, B., Shen, Q.H., et al., 1988. Archean crustal evolution in China: the Taishan complex, and evidence for Juvenile crustal addition from long-term depleted mantle. Precambrian Research 38, 381–403.

Jahn, B.M., Wu, F.Y., Lo, C.-H., Tsai, C.H., 1999. Crust-mantle interaction induced by deep subduction of the continental crust: Geochemical and Sr–Nd isotopic evidence from post-collisional mafic-ultramafic intrusions of the northern Dabie complex, central China. Chemical Geology 157, 119–146.

Jiang, L.L., Liu, Y.C., Wu, W.P., Su, W., 1999. Deformation history and exhumation process of ultrahigh pressure metamorphic rocks in Dabie Mt. Geological Sciences 34, 432–441 (in Chinese with English abstract).

Kay, R.W., Kay, S.M., 2002. Andean adakites: three ways to make them. Acta Petrologica Sinica 18, 303–311 (in Chinese with English abstract).

Leake, B.E., Woolley, A.R., Arps, C.E.S., Birch, W.D., Gilbert, M.C., Grice, J.D., Hawthorne, F.C., Kato, A., Kisch, H.J., Krivovichev, V.G., Linthout, K., Laird, J., Mandarino, J.A., Maresch, W.V., Nickel, E.H., Rock, N.M.S., Schumacher, J.C., Smith, D.C., Stephenson, N.C.N., Ungaretti, L., Whittaker, E.J.W., Guo, Y., 1997. Nomenclature of amphiboles: report of the subcommittee on amphiboles of the International Mineralogical Association, Commission on New Minerals and Mineral Names. American Mineralogist 82, 1019–1037.

Li, S.G., Harte, S., Zheng, S., Liu, D., Zhang, G., Guo, A., 1989. Timing of collision between the North and South China blocks—The Nm–Nd isotopic age evidence. Science in China, Series B 32, 1393–1400.

Li, S.G., Nie, Y.H., Hart, S.R., Zheng, S.G., 1998. Upper mantle-deep subducted continental crust interaction: (II) Sr and Nd isotopic constraints on the syn-collisional mafic to ultramafic intrusions in the northern Dabieshan, eastern China (in Chinese). Science in China, Series D 28, 18–22.

Li, Z.X., Li, X.H., Kinny, P.D., 1999. The breakup of Rodinia: did it start with a mantle plume beneath South China? Earth and Planetary Science Letters 173, 171–181.

Lin, J., Tang, D., Li, J., Liu, Z., 2000. Early Jurassic Banjing intrusive complex of southern marginal zone of the North China block, Xuzhou. Journal of Changchun University of Science and Technology 30, 209–214 (in Chinese with English abstract).

Liu, Y., Liu, H.C., Li, X.H., 1996. Simultaneous and precise determination of 40 trace elements in rock samples using ICP-MS. Geochemica 25, 552–558 (in Chinese with English abstract).

Luo, Z.K., Miao, L.C., 2002. Granites and gold deposits in Zhaoyuan–Laizhou area, eastern Shandong province. Metallurgical Industry Press, Beijing pp. 20–57 (in Chinese).

Ma, X., Bai, J., 1998. Precambrian crustal evolution of China. Geological Publication House, Springer, Berlin pp. 1–331.

Pan, G.Q., Lu, X.C., Yu, H.B., 2001. Petrological and geochemical characteristics of Mesozoic adakite from Northern Huaiyang and discussion on its genesis. Acta Petrologica Sinica 17, 541–550 (in Chinese with English abstract).

Petford, N., Atherton, M.P., 1996. Na-rich partial melts from newly underplated basaltic crust: the Cordillera Blanca Batholith. Peru Journal of Petrology 37, 1491–1521.

Qiao, G.-S., Wang, K.-Y., Guo, Q.-F., Zhang, G.-C., 1987. Sm–Nd dating of Caozhuang early Archean supercrustals, Eastern Hebei. Scientia Geologica Sinica 22, 86–92 (in Chinese with English abstract).

Qiao, G.-S., Zhai, M.-G., Yan, Y.-H., 1990. Geochronological study of Archean rocks in Anshan, Liaoning Province. Scientia Geologica Sinica 25, 158–165 (in Chinese with English abstract).

Rapp, R.P., Watson, E.B., 1995. Dehydration melting of metabasalt at 8–32 Kbar: implications for continental growth and crust-mantle recycling. Journal of Petrology 36, 891–931.

Rapp, R.P., Shimizu, N., Norman, M.D., Applegate, G.S., 1999. Reaction between slab-derived melts and peridotite in the mantle wedge: experimental constraints at 3.8 GPa. Chemical Geology 160, 335–356.

Rapp, R.P., Long, X., Shimizu, N., 2002. Experimental constraints on the origin of potassium-rich adakites in eastern China. Acta Petrologica Sinica 18, 293–302 (in Chinese with English abstract).

Wang, Q.C., Lin, W., 2002. Geodynamics of the Dabieshan collisional orogenic belt. Earth Science Frontiers 9, 257–265 (in Chinese with English abstract).

Wang, G., Jiang, B., Cao, D., Zhou, H., 1998. On the Xuzhou–Suzhou arcuate duplex-imbricate fan thrust system. Acta Geologica Sinica 72, 228–236 (in Chinese with English abstract).

Wu, F., Sun, D., 1999. The Mesozoic magmatism and lithospheric thinning in eastern China. Journal of Changchun University of Science and Technology 29, 313–318 (in Chinese with English abstract).

Xu, W.L., Wang, D.Y., Wang, S.M., 2000. PTtC model of Mesozoic and Cenozoic volcanism and lithospheric evolution. Journal of Changchun University of Science and Technology 30, 329–335 (in Chinese with English abstract).

Xu, J.F., Wang, Q., Xu, Y.G., Zhao, Zh., Xiong, X.L., 2001. Geochemistry of Anjishan intermediate-acid intrusive rocks in Ningzhen area: Constraint to origin of the magma with HREE and Y depletion. Acta Petrologica Sinica 17, 576–584 (in Chinese with English abstract).

Xu, J.F., Shinjo, S., Defant, M.J., Wang, Q., Rapp, R.P., 2002a. Origin of Mesozoic adakitic intrusive rocks in the Ningzhen area of east China:

partial melting of delaminated lower continental crust. Geology 30, 1111–1114.

Xu, W.L., Wang, D.Y., Liu, X.C., Wang, Q.H., Lin, J.Q., 2002b. Discovery of eclogite inclusions and its geological significance in early Jurassic intrusive complex in Xuzhou-northern Anhui, eastern China. Chinese Science Bulletin 47, 1212–1216.

Xu, W.L., Wang, Q.H., Liu, X.C., Wang, D.Y., Guo, J.H., 2004a. Chronology and sources of Mesozoic intrusive complex in Xu-Huai region, central China: Constraints from SHRIMP zircon U–Pb dating. Acta Geologica Sinica 78, 96–106.

Xu, W.L., Wang, Q.H., Wang, D.Y., Pei, F.P., Gao, S., 2004b. Processes and mechanism of Mesozoic lithospheric thinning in eastern North China Craton: evidence from Mesozoic igneous rocks and deep-seated xenoliths. Earth Science Frontiers 11, 309–317 (in Chinese with English abstract).

Xu, W.L., Wang, Q.H., Liu, X.C., Guo, J.H., 2005. SHRIMP zircon U–Pb dating in Jingshan 'migmatitic granite', Bengbu and its geological significance. Science in China, Series D 48, 185–191.

Yang, J.S., Xu, Z.Q., Wu, C.L., Liu, F.L., Shi, R.D., Wooden, J., 2002. SHRIMP U–Pb dating on coesite-bearing zircon: evidence for Indosinian ultrahigh-pressure metamorphism in Su–Lu, east China. Acta Geologica Sinica 76, 354–372 (in Chinese with English abstract).

Zhang, Q., Wang, Y., Qian, Q., Yang, J., Wang, Y.L., Zhao, T.P., Guo, G.J., 2001. The characteristics and tectono-metallogenic significance of the adakites in Yanshan period from eastern China. Acta Petrologica Sinica 17, 236–244 (in Chinese with English abstract).

Zhao, G., Wilde, S.A., Cawood, P.A., Sun, M., 2001. Archean blocks and their boundaries in the North China craton: lithological, geochemical, structural and P–T path constraints and tectonic evolution. Precambrian Research 107, 45–73.

Zheng, Y., Fu, B., Gong, B., Li, L., 2003. Stable isotope geochemistry of ultrahigh pressure metamorphic rocks from the Dabie-Sulu orogen in China: Implications for geodynamics and fluid regime. Earth Science Review 62, 105–161.